## Princeton Plasma Physics Laboratory

PPPL- 4675

PPPL- 4675

# Stress Multipliers for the NSTX Upgrade Digital Coil Protetion System

P.H. Titus, R. Woolley, R. Hatcher

September, 2011

Prepared for the U.S. Department of Energy under Contract DE-AC02-09CH11466.

# Stress Multipliers for the NSTX Upgrade Digital Coil Protection System

*Peter H. Titus, R. Woolley, R. Hatcher*
Princeton Plasma Physics Laboratory, Princeton, NJ 08543-0451 USA
ptitus@pppl.gov

***Abstract*—Conceptual design of the upgrade to NSTX, explored designs sized to accept the worst loads that power supplies could produce. This produced excessive structures that would have been difficult to install and were much more costly than needed to meet the scenarios required for the upgrade mission. Instead, the project decided to rely on a digital coil protection system (DCPS). Initial sizing was then based on the 96 scenarios in the project design point with some headroom to accommodate operational flexibility and uncertainty. This has allowed coil support concepts that minimize alterations to the existing hardware. The digital coil protection system theory , hardware and software are described in another paper at this conference. The intention of this paper is to describe the generation of stress multipliers, and algorithms that are used to characterize the stresses at key areas in the tokamak, as a function of either loads calculated by the influence coefficients computed in the DCPS software, or directly from the coil currents.**

***Keywords-component; NSTX; Influence Coefficients; Polidal Field Coils (key words)***

## I. Introduction

Two approaches are used to provide the needed multipliers/algorithms. The first is to use the loads on PF coils computed by the DCPS software and apply these to local models of components. This works well for coil supports and for uniformly supported coils. It is usual practice to utilize influence coefficient calculations to determine hoop and axial (vertical for tokamak's) loads from coil currents. However the centroid of the Lorentz loads may not be at the geometric center of the coils. Where there is significant offset between the Lorentz centroid and the geometric center, there will be a moment about the coil geometric center in addition to the net loads. This may be a significant contributor to the support reaction loads and to the stresses in the coils. In design and analysis of coil systems, distributions of fields and forces are typically calculated for a useful structural/magnetic mesh which is typically fine enough to properly distribute the Lorentz forces and resolve any moments about the coil current centers. When influence coefficients are used in control systems, for operating tokamaks, to check coil stresses and support loading, the effect of moments has been omitted. To the author's knowledge, this is true of Alcator C-Mod, TFTR and NSTX . Addition of the moment coefficients completes the three degrees of freedom available from the axisymmetric analysis of ring coils.

The second approach to calculating the stress multipliers/algorithms, is to utilize a global model that simulates the whole structure and includes an adequately refined modeling of the component in question. Unit terminal currents are applied to each coil separately, Lorentz Loads calculated, and the response of the whole tokamak and local component stress is computed. For superposition to work, stress multipliers must be computed for specific locations and individual stress components (not equivalent, von Mises, or Tresca) must be calculated. Results for two components are presented after the discussion of moment coefficients.

## II. Computation of Influence Coefficients Including Moment Coefficients

### A. *Utility of Moment Coefficients*

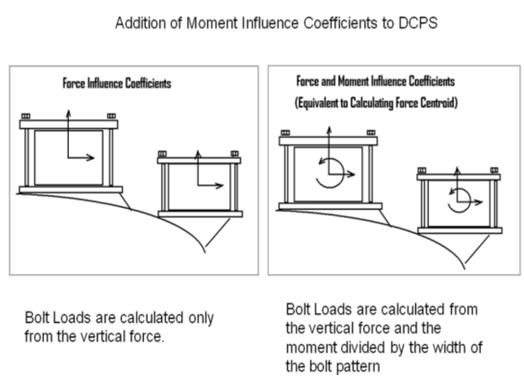


Figure 1. Representation of Applied Forces and Moments on Coils

In the example in figure 1, at left, the retainer bolts would simply be stressed by the vertical loading, and at right the bolts would see the vertical load plus a force equal to the moment divided by the clamp bolt spacing. Obviously more complex structural innteractions are possible, and for the coil aspect ratios shown, there will not be a large difference between the current and geometric centers. Other coil shapes and magnetic configurations may see larger effects from calculated moments. For NSTX Upgrade the inner PF coils are effected significantly by moments.

Work was performed under DOE Contract No. DE-AC02-09CH11466

*B. The Analysis Code*

Mesh generation , calculation of the Lorentz forces, and generation of the influence coefficients is done using a code written by the author of this report. The mesh generation feature of the code is checked visually and within ANSYS during the PREP7 geometry check. . The authors code uses elliptic integrals for 2D field calculations, and Biot Savart solution for 3D field calculations. These are based 2D formulations, and single stick field calculations from ref.R [1] with some help from R. Pillsbury's FIELD3D code to catch all the coincident current vectors, and other singularities.

The code in various forms has been used for 20 years and is suitable for structural calculations. It is also being used for calculation of load files in an NSTX global model[9]. Recent checks include NSTX out-of-plane load comparisons with ANSYS [10] and MAXWELL and calculations of trim coil fields for W7X compared with N. Pomphrey's calculations. Some information on the code, named FTM (Win98) and NTFTM2 (NT,XP), is available at: http://198.125.178.188/ftm/manual.pdf ). or, within PPPL: at P:\public\Snap-srv\Titus\NTFTM

*C. The Axisymmetric Model*

The influence coefficient methodology allows choice of coil groups or partial coil groups with which to construct the influence coefficient matrices. This also allows odd shaped coil segments or shaped or shifted plasmas that are treated simply as another coil group by the program. Computation of influence coefficients is done by computing contributions of fields and forces in one element group with respect to other element groups. The element groups are identified by member element real constant numbers. For this paper, the element designations used by R. Hatcher's calculation [2] have been used to allow a comparison with other calculated force influence coefficients..

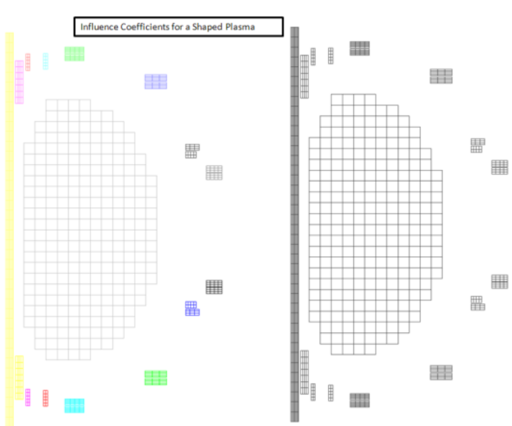


Figure 2. Axisymmetric Model Used to Compute Influence Coefficients. At Left, Colors Represent Real Constant Assignments

Moment coefficients require the computation of the force contributions with a running summation of forces multiplied by the element force times the appropriate radial or axial lever arm with respect to the element group centroid. Computation of the moment influence coefficients also produces the force influence coefficients. Figure 2 shows a coil and plasma mesh used for computation of the influence coefficients tabulated in this paper. Two plasma shapes have been investigated a rectangular cross section and a shaped plasma. The shaped plasma is shown in figure 2. Tabulated influence coefficients are for the rectangular plasma.

| | (cm) | (cm) | (cm) | (cm) | | | | 0 |
|---|---|---|---|---|---|---|---|---|
| OH (half-plane) | 24.2083 | 6.934 | 106.04 | 212.08 | 4 | 110 | 442 | 0.701 |
| PF1a | 32.4434 | 6.2454 | 159.06 | 46.3296 | 4 | 16 | 64 | 0.825 |
| PF1b | 40.038 | 3.36 | 180.42 | 18.1167 | 2 | 16 | 32 | 0.794 |
| PF1c | 55.052 | 3.7258 | 181.36 | 16.6379 | 2 | 10 | 20 | 0.856 |
| PF2a | 79.9998 | 16.271 | 193.3473 | 6.797 | 7 | 2 | 14 | 0.741 |
| PF2b | 79.9998 | 16.271 | 185.26 | 6.797 | 7 | 2 | 14 | 0.741 |
| PF3a | 149.446 | 18.644 | 163.3474 | 6.797 | 7.5 | 2 | 15 | 0.693 |
| PF3b | 149.446 | 18.644 | 155.26 | 6.797 | 7.5 | 2 | 15 | 0.693 |
| PF4b | 179.4612 | 9.1542 | 80.7212 | 6.797 | 2 | 4 | 8 | 0.753 |
| PF4c | 180.6473 | 11.527 | 88.8086 | 6.797 | 4.5 | 2 | 9 | 0.672 |
| PF5a | 201.2798 | 13.533 | 65.2069 | 6.858 | 6 | 2 | 12 | 0.773 |
| PF5b | 201.2798 | 13.533 | 57.8002 | 6.858 | 6 | 2 | 12 | 0.773 |

```
rcoi
16
1,10,80,884,250    !OH
2,4,7,64,250       !PF1AU
3,2,5,32,250       !PF1bU
4,2,5,20,250       !PF1c
5,4,10,28,250
6,3,10,30,250
7,1,17,17,250
8,4,6,24,250
9,4,7,64,250
10,2,5,32,250
11,2,5,20,250
12,4,10,28,250
13,3,10,30,250
14,1,17,17,250
15,4,6,24,250
16,6,8,1,250
```

Figure 3. Coil Builds for NSTX Upgrade

Coil builds for the NSTX Upgrade are shown in Figure 3. in the table at left. At right, the commands used to apply the unit currents are shown. In this case one kiloamp is the unit current, but 250 amps is input because subsequently the mesh density is increased by a factor of 4.

*D. Results*

A full set of force and moment influence coefficients are included near the end of this paper.

*E. A Test Case*

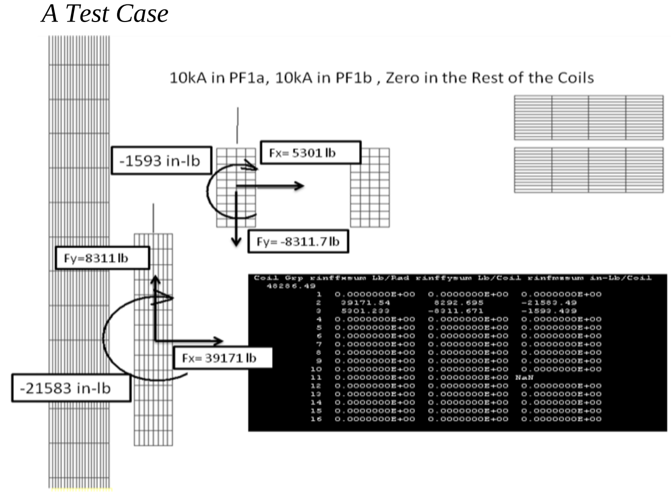


Figure 4. Upper Inner Corner of the NSTX Poloidal Field Coil Array

For NSTX the effect of the moment coefficients is small for the compact ring coils but is interesting for the thin solenoids - the OH and PF1a,b,and c. In Figure 4, The upper inner portion of the NSTX PF coil array is shown This includes an upper segment of the tall thin OH and PF1 a,b and c. The staggered coils will develop current centers that aren't coincident with their geometric centers. For the case with

10kA  in PF1a and 10kA in Pf1b, the forces and moments are shown.

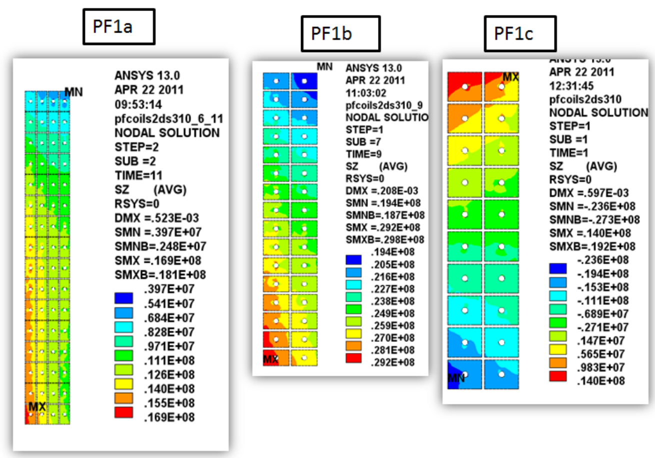


Figure 5. Inner PF Coil Results from [6]

Stress analysis of the inner PF coils performed for NSTX upgrade showed a strong variation in the vertical distribution of hoop stress in PF 1a and b similar to the behavior shown in the test case. Figure 5 shows some results from the qualification of the inner PF coils, in [6]

TABLE I. EXCERPT FROM THE SHAPED PLASMA MOMENT INFLUENCE COEFFICIENTS

| | | OH | PF1AU | PF1bU | PF1cU | PF2U | PF3U | PF4U |
|---|---|---|---|---|---|---|---|---|
| OH | 1 | 0.00E+00 | -20165.7 | -9837.4 | -5246.08 | -5607.03 | -3893.17 | -1291.17 |

| PF5U | PF1AL | PF1bL | PF1cL | PF2L | PF3L | PF4L | PF5L | Ip |
|---|---|---|---|---|---|---|---|---|
| -1209.61 | 20165.75 | 9837.401 | 5246.083 | 5607.024 | 3893.168 | 1291.17 | 1209.613 | 1.582384 |

The largest moment influence factors are for moments on the OH from PF1aU and L currents as might be expected from the coil geometries. The effect on the outer ring coils is minimal. The results of this calculation were compared with R. Hatchers results for the 2009 coil builds and with R. Woolley's calculations for the 2011 coil builds. The comparison with Wooley's moment coefficients show results typically within 2 to 5 % with two outliers at 8%, and large difference ratios when the two analyses are both calculating essentially zero factors.

## III. TF INNER LEG STRESS INFLUENCE COEFFICIENTS USING THE TOKAMAK GLOBAL MODEL RESULTS WITH UNIT CURRENTS APPLIED

### *A. Methodology*

Out-of-Plane (OOP) loads on a toroidal field (TF) coil system result from the cross product of the poloidal field and toroidal field coil current. Support of OOP loads is statically in-determinant, or multiply redundant, requiring an understanding of the flexibility of the outboard structures and the inboard stiffness of the central column. There are a number of ways in which the torsional shear stress in the inner leg of the TF can be calculated. The global model is the primary tool for this computation. A single TF cyclic symmetry model was investigated to see if the inner leg OOP forces alone dominate and if the outer structures could be ignored. This turned out not to be the case. This means that the global torsional stiffness's of all the tokamak structures, the umbrella structure, it's proposed upgrade reinforcements, the port region stiffness, the top and bottom spoked lid assembly stiffness, and the pedestal stiffness, all will have some effect on the inner leg torsional shear.

The global model was run with full TF current and 1000kA of current in each PF coil. The influence coefficients are based on 1 kA, but it was expected that TF loading might overwhelm the loads from individual smaller coils. The model is linear and the stress due to the PF loads should be fully scalable by current. The influence coefficients are corrected in the spreadsheet. The force calculations are computed and applied to the global model. The torsional shear in the upper, middle, and lower inner leg were then determined from each of the 16 load cases that resulted.

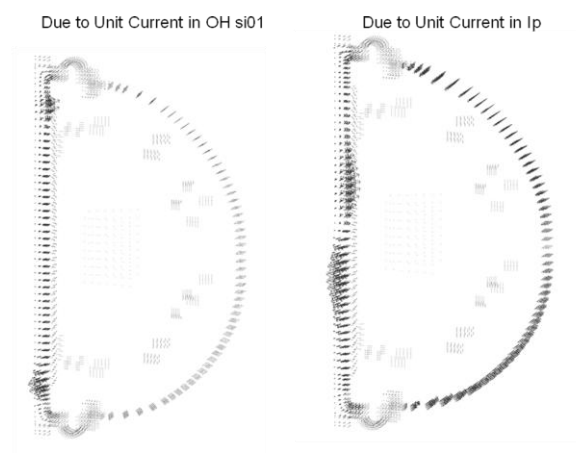


Figure 6. Detailed Model of PF4/5 with Equatorial Plane Symmetry

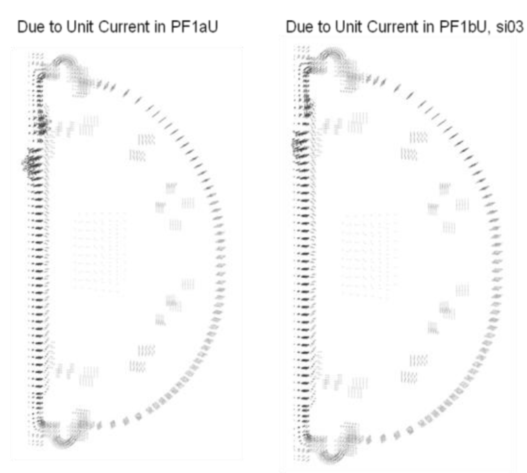


Figure 7. PF5 "Smeared" Coil Bending Stress.

## *B. Results*

Based on the DCPS influence coefficient TF inner leg upper corner torsional shear, for all 96 June 3 2010 scenarios are all below 20 MPa with and without plasma. Rigorously these should have the 10% headroom applied (the coefficients do not include this) - Consequently, the torsional shear stress to compare with the allowable is 22 MPa. Acceptable results from testing the CTD-101K/Cyanate Ester primer system[7], Indicate that the torsional shear is acceptable. Influence coefficients for the DCPS algorithm have been generated based on the global model [2].

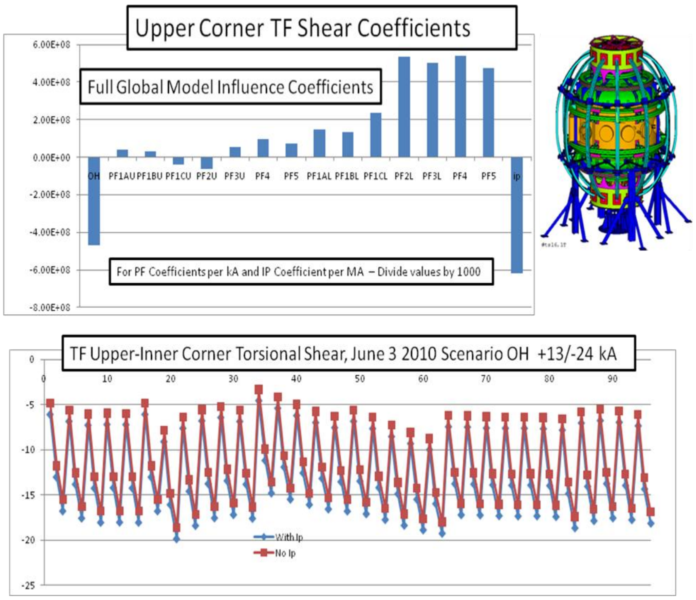


Figure 8. Upper TF Torsional Shear Stress Multipliers and Results for the Project's 96 Equilibria, with and without plasma

## IV. Computation of PF Conductor Hoop Stress Stress Multipliers

### *A. Approach for Calculation PF Stress Multipliers*

The approach used for the PF4 and 5 coils for calculating the stress multipliers/algorithms is to utilize a global model (same as shown for the TF torsional shear coefficients) that simulates the whole structure and includes an adequately refined modeling of the component in question. As in the TF torsional shear stress multipliers, a limited number of sections must be identified from an understanding of the results for likely critical locations. This is done by evaluating results for the 96 design scenarios for NSTX.

### *B. PF5 Hoop Stress Multiplier*

Unit terminal currents are applied to each coil separately, paired with PF5 Lorentz loads are calculated, and the response of the whole tokamak and local component stress is computed. Figure 10 shows a Biot Savart computation with unit loads in PF4 and 5.

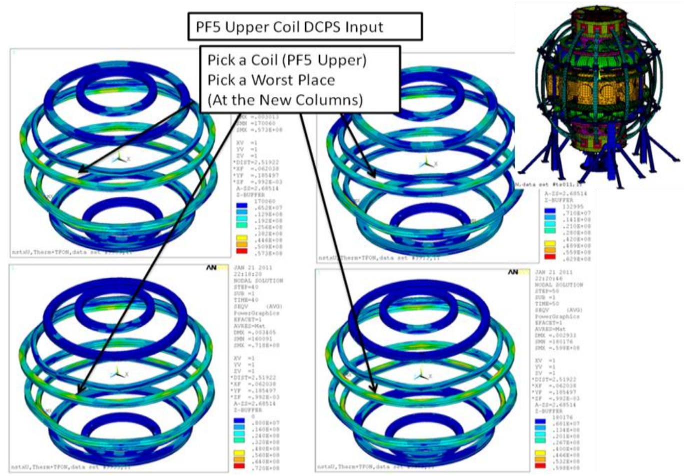


Figure 9. "Smeared" PF Coil Bending Stress From the Global Model.

This approach is correct for stresses that are a consequence of an individual coil load which is in turn a result of the superposition of contributions from all other coil currents. Local component stresses may then be computed in the DCPS or in a spreadsheet for the many scenarios required by the GRD. This approach has been applied to the PF4 and 5 coil stress. Where a component stress is a consequence of multiple coil loads, the approach must derive coefficients from unit loads which in turn are computed from the influence coefficients.

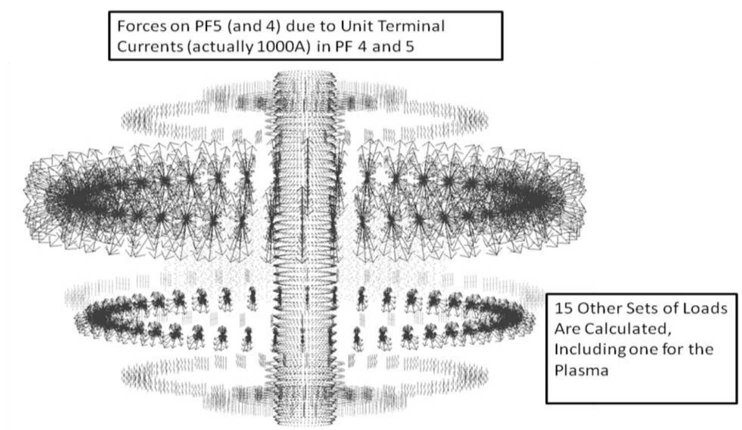


Figure 10. Lorentz Loads for a Unit Terminal Currents for PF4 and 5

Figure 8 shows the Lorentz forces for the interaction between PF4 and 5 with unit currents. Loading for interactions between PF 5 and the rest of the 16 coil set that defines the NSTX poloidal coil system are computed.

*C. Identify the Headings*

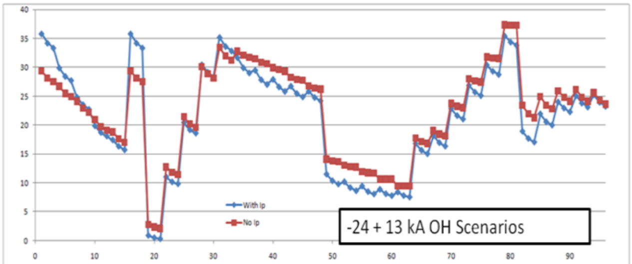


Figure 11. PF5 "Smeared" Coil Bending Stress.

"Smeared" results are determined from the influence coefficients. A more detailed model is used to calculate the local stress in the conductor and insulator. The load case in the detailed model is the full current in PF4 and 5 and is up-down symmetric. This must be used to estimate the local stresses for 96 designs scenarios, and operational currents in the DCPS.

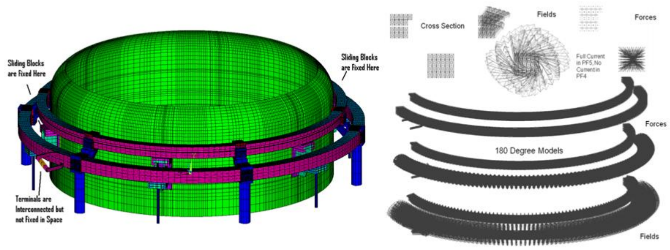


Figure 12. Detailed Model of PF4/5 with Equatorial Plane Symmetry

To form a basis of comparison between the influence coefficient calculations based on "smeared" results, and the detailed model, the influence coefficients were applied to the PF 4/5 up-down symmetric analysis used for the detailed model.

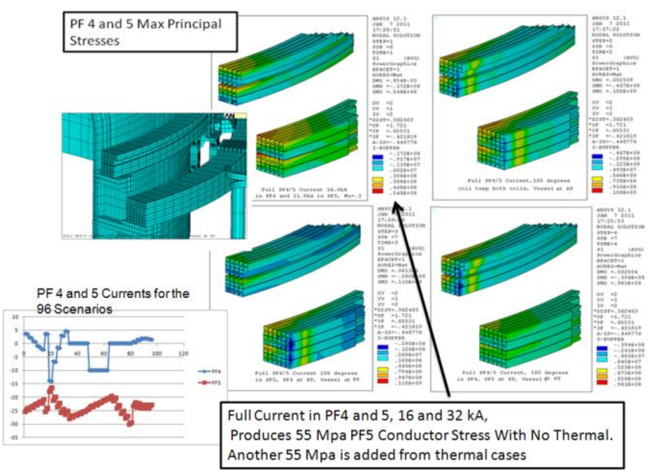


Figure 13. Local Conductor Stresses from the Detailed Model Shown in Figure 10.

In addition to the Lorentz force loads on the coils, there are thermal stresses that result from constraints of the thermal expansion of the coil needed to maintain concentricity of the coil centers (control the n=1 error while allowing n=2 errors) This constitutes an additional 55 MPa in the conductor max principal stress that adds to the values from the Lorentz loading. Stress results for the detailed model are shown in fig. 13.

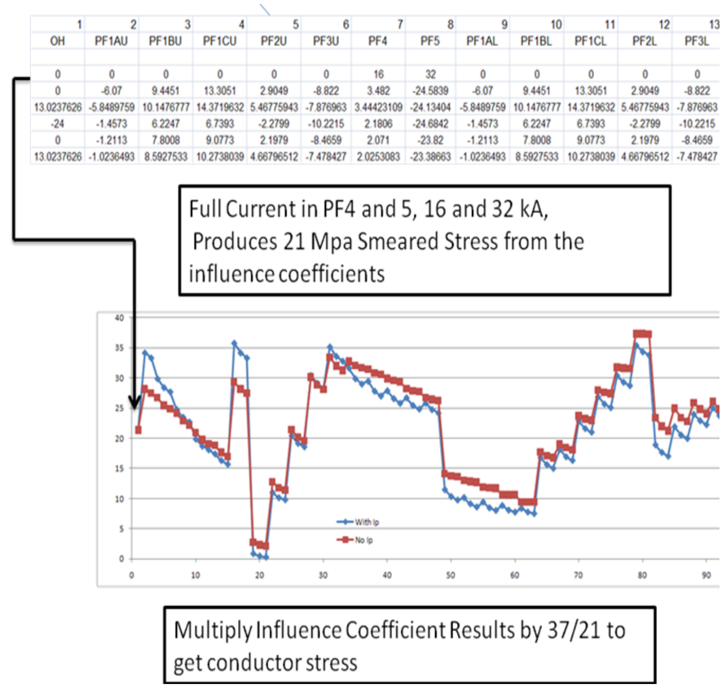

| 1 | 2 | 3 | 4 | 5 | 6 | 7 | 8 | 9 | 10 | 11 | 12 | 13 |
|---|---|---|---|---|---|---|---|---|---|---|---|---|
| OH | PF1AU | PF1BU | PF1CU | PF2U | PF3U | PF4 | PF5 | PF1AL | PF1BL | PF1CL | PF2L | PF3L |
| | | | | | | | | | | | | |
| 0 | 0 | 0 | 0 | 0 | 0 | 16 | 32 | 0 | 0 | 0 | 0 | 0 |
| 0 | -6.07 | 9.4451 | 13.3051 | 2.9049 | -8.822 | 3.482 | -24.5839 | -6.07 | 9.4451 | 13.3051 | 2.9049 | -8.822 |
| 13.0237626 | -5.8489759 | 10.1476777 | 14.3719632 | 5.46775943 | -7.876963 | 3.44423109 | -24.13404 | -5.8489759 | 10.1476777 | 14.3719632 | 5.46775943 | -7.876963 |
| -24 | -1.4573 | 6.2247 | 6.7393 | -2.2799 | -10.2215 | 2.1806 | -24.6842 | -1.4573 | 6.2247 | 6.7393 | -2.2799 | -10.2215 |
| 0 | -1.2113 | 7.8008 | 9.0773 | 2.1979 | -8.4659 | 2.071 | -23.82 | -1.2113 | 7.8008 | 9.0773 | 2.1979 | -8.4659 |
| 13.0237626 | -1.0236493 | 8.5927533 | 10.2738039 | 4.66796512 | -7.478427 | 2.0253083 | -23.38663 | -1.0236493 | 8.5927533 | 10.2738039 | 4.66796512 | -7.478427 |



Figure 14. Influence Coefficients Calculation Including One Data Point at the PF4/5 Full Coil Current Case Used in the Detailed Analysis .

The ratio of the detailed model results divided by the smeared influence coefficient results was found to be 37/21 or 1.76 . This is then used as a part of the DCPS algorythm by additionally applying this factor to teh influence coefficients to obtain the PF5 Lorentz hoop stress for the current operating condition.

## V. Conclusion

NSTX Upgrade is planning to implement the Digital Coil Protection System or DCPS. It is an extensive system of computer and power supply controls intended protect the coils and support structures. During the NSTX Upgrade design phase a number of algorithms have been developed to predict stresses in critical components of the tokamak. Addition of moment influence coefficients to the usual set of radial and axial force influence coefficients has been described. Specific stress multipliers based on unit currents have been described in this paper. Initial operation of the DCPS and tokamak operation will test the utility and accuracy of these stress simulations. When the full complexity of all the component stress checks is implemented, and de-bugged, the DCPS should become a useful tool for shot planning, and machine protection.

TABLE II. **INFLUENCE COEFFICIENTS IN SI UNITS**

| | | OH | PF1AU | PF1bU | PF1cU | PF2U | PF3U | PF4U | PF5U | PF1AL | PF1bL | PF1cL | PF2L | PF3L | PF4L | PF5L | Ip |
|---|---|---|---|---|---|---|---|---|---|---|---|---|---|---|---|---|---|
| FX | | Influence | Matrix | N/rad | | | | | | | | | | | | | |
| OH | 1 | 25230.3 | 3806.061 | 1708.908 | 967.1191 | 1134.092 | 1209.182 | 776.9004 | 1080.26 | 3806.043 | 1708.914 | 967.123 | 1134.096 | 1209.203 | 776.8887 | 1080.252 | 58.04883 |
| PF1AU | 2 | -140.673 | 856.7656 | 804.679 | 402.8212 | 385.0967 | 267.9286 | 97.79694 | 113.873 | 2.693542 | 1.662048 | 1.908569 | 5.065918 | 19.87793 | 25.48993 | 46.92737 | 1.891357 |
| PF1bU | 3 | -111.435 | -147.157 | 344.059 | 462.4921 | 333.3344 | 164.4536 | 52.2583 | 60.96289 | 1.346069 | 0.843353 | 0.970917 | 2.600311 | 10.30087 | 13.1109 | 24.38876 | 0.834534 |
| PF1cU | 4 | -49.8817 | -66.3434 | -186.161 | 152.8504 | 363.0069 | 147.4613 | 44.34793 | 51.61908 | 1.111908 | 0.69957 | 0.805283 | 2.161407 | 8.583679 | 10.90804 | 20.36479 | 0.65506 |
| PF2U | 5 | -31.1968 | -44.1531 | -82.4588 | -136.834 | 292.1378 | 317.2212 | 81.96744 | 95.94821 | 1.96759 | 1.253113 | 1.443481 | 3.899963 | 15.58963 | 19.65652 | 37.01328 | 1.009399 |
| PF3U | 6 | -21.5523 | -26.2723 | -19.4406 | -24.8062 | -74.7123 | 400.619 | 163.52 | 198.7234 | 3.382355 | 2.227905 | 2.566162 | 7.052979 | 28.73105 | 35.6076 | 68.99472 | 0.94574 |
| PF4U | 7 | -14.8351 | -3.98004 | -1.31325 | -1.43192 | -0.89291 | 16.79922 | 150.6147 | 444.4194 | 2.456009 | 1.717377 | 1.986237 | 5.62558 | 23.96396 | 30.02812 | 62.74477 | -0.35266 |
| PF5U | 8 | -20.3084 | -2.72794 | -0.53848 | -0.5621 | 1.093414 | 15.20554 | -199.776 | 300.6638 | 2.999451 | 2.246582 | 2.606537 | 7.632538 | 33.50699 | 39.08331 | 86.71771 | -1.09036 |
| PF1AL | 9 | -140.673 | 2.693604 | 1.662109 | 1.908752 | 5.066101 | 19.87787 | 25.4903 | 46.92773 | 856.7654 | 804.6786 | 402.821 | 385.0972 | 267.929 | 97.79706 | 113.8729 | 1.891724 |
| PF1bL | 10 | -111.435 | 1.3461 | 0.843353 | 0.970947 | 2.600433 | 10.30093 | 13.11102 | 24.38889 | -147.157 | 344.0589 | 462.4922 | 333.3345 | 164.4537 | 52.25842 | 60.96298 | 0.834717 |
| PF1cL | 11 | -49.8816 | 1.111908 | 0.699554 | 0.805328 | 2.161484 | 8.583694 | 10.90807 | 20.36481 | -66.3433 | -186.161 | 152.8504 | 363.007 | 147.4612 | 44.34799 | 51.61909 | 0.655121 |
| PF2L | 12 | -31.1969 | 1.96756 | 1.253174 | 1.443481 | 3.900024 | 15.58957 | 19.65646 | 37.01309 | -44.1531 | -82.459 | -136.834 | 292.1379 | 317.2212 | 81.9675 | 95.9483 | 1.00943 |
| PF3L | 13 | -21.5522 | 3.382446 | 2.227753 | 2.566376 | 7.05304 | 28.73096 | 35.6077 | 68.99469 | -26.2725 | -19.4405 | -24.8061 | -74.7123 | 400.6189 | 163.5198 | 198.7233 | 0.945801 |
| PF4L | 14 | -14.8352 | 2.456024 | 1.717377 | 1.986221 | 5.625595 | 23.96391 | 30.02812 | 62.74481 | -3.97992 | -1.31326 | -1.43192 | -0.89294 | 16.79919 | 150.6147 | 444.4194 | -0.35263 |
| PF5L | 15 | -20.3084 | 2.999481 | 2.246521 | 2.606598 | 7.632538 | 33.50702 | 39.0834 | 86.7178 | -2.72781 | -0.53839 | -0.56195 | 1.093506 | 15.20557 | -199.776 | 300.6637 | -1.09033 |
| Ip | 16 | -0.65479 | 0.39844 | 0.250672 | 0.287969 | 0.757769 | 2.9888 | 4.106287 | 6.647198 | 0.39844 | 0.250672 | 0.287969 | 0.757769 | 2.9888 | 4.106287 | 6.647198 | 0.205512 |

| FY | | Influence | Matrix | N/rad | | | | | | | | | | | | | |
|---|---|---|---|---|---|---|---|---|---|---|---|---|---|---|---|---|---|
| OH | 1 | 0.00E+00 | 101.6216 | 132.1296 | 87.8682 | 115.5602 | 56.18751 | 13.25849 | 12.59733 | -101.621 | -132.129 | -87.8677 | -115.56 | -56.1874 | -13.2583 | -12.5974 | 1.15E-04 |
| PF1AU | 2 | -101.118 | 0.00E+00 | 384.1478 | 118.9599 | 77.54909 | 0.139336 | -8.96284 | -10.4976 | -0.15052 | -9.56E-02 | -0.14978 | -0.4568 | -2.08736 | -2.97952 | -5.23168 | -0.41885 |
| PF1bU | 3 | -131.409 | -386.426 | 0.00E+00 | 13.84991 | 35.47831 | -9.61017 | -7.17572 | -7.91616 | -9.66E-02 | -6.30E-02 | -9.43E-02 | -0.28422 | -1.29785 | -1.85637 | -3.34522 | -0.21371 |
| PF1cU | 4 | -87.757 | -119.389 | -13.8709 | 0.00E+00 | 67.80286 | -13.4356 | -8.80649 | -9.60769 | -0.14898 | -9.25E-02 | -0.12476 | -0.35941 | -1.56134 | -2.19689 | -3.96695 | -0.23739 |
| PF2U | 5 | -115.714 | -77.7934 | -35.61 | -68.2043 | 0.00E+00 | -69.1412 | -26.9411 | -28.6129 | -0.45662 | -0.28304 | -0.36006 | -1.00674 | -4.25728 | -5.93188 | -10.8552 | -0.55093 |
| PF3U | 6 | -56.2119 | -0.1395 | 9.6224 | 13.45625 | 69.21666 | 0.00E+00 | -157.733 | -149.975 | -2.08676 | -1.29659 | -1.56193 | -4.25708 | -17.5993 | -24.5514 | -46.0942 | -1.64419 |
| PF4U | 7 | -13.2569 | 8.966514 | 7.175429 | 8.808064 | 26.94148 | 157.7714 | 0.00E+00 | -368.7 | -0.83501 | 0.288889 | -5.35E-02 | -3.78803 | -22.4096 | -33.9093 | -67.3666 | 0.65353 |
| PF5U | 8 | -12.5961 | 10.50075 | 7.915802 | 9.609217 | 28.61358 | 149.9904 | 371.0913 | 0.00E+00 | -5.23136 | -3.34403 | -3.96774 | -10.8557 | -46.0978 | -69.5098 | -140.886 | -1.53568 |
| PF1AL | 9 | 101.1179 | 0.150541 | 9.56E-02 | 0.149777 | 0.456797 | 2.08738 | 2.979534 | 5.231685 | 0.00E+00 | -384.148 | -118.96 | -77.5491 | -0.13934 | 8.962835 | 10.49761 | 0.418849 |
| PF1bL | 10 | 131.4086 | 9.55E-02 | 6.19E-02 | 9.32E-02 | 0.283148 | 1.296791 | 1.855291 | 3.344139 | 386.4264 | 0.00E+00 | -13.8499 | -35.4783 | 9.61014 | 7.175722 | 7.916151 | 0.213699 |
| PF1cL | 11 | 87.75694 | 0.149756 | 9.33E-02 | 0.125511 | 0.360171 | 1.562139 | 2.197661 | 3.967718 | 119.3888 | 13.87093 | 0.00E+00 | -67.8029 | 13.43558 | 8.80649 | 9.607681 | 0.23738 |
| PF2L | 12 | 115.7142 | 0.456672 | 0.283127 | 0.360149 | 1.00679 | 4.257355 | 5.931921 | 10.85529 | 77.79339 | 35.61006 | 68.20438 | 0.00E+00 | 69.14127 | 26.94106 | 28.61289 | 0.550955 |
| PF3L | 13 | 56.21167 | 2.086667 | 1.296516 | 1.561787 | 4.257044 | 17.59918 | 24.55125 | 46.09405 | 0.139395 | -9.62249 | -13.4564 | -69.2168 | 0.00E+00 | 157.7327 | 149.9749 | 1.644278 |
| PF4L | 14 | 13.25691 | 2.97919 | 1.855294 | 2.19768 | 5.932143 | 24.55371 | 36.0535 | 69.51076 | -8.96656 | -7.17546 | -8.80807 | -26.9415 | -157.772 | 0.00E+00 | 368.6999 | -0.65354 |
| PF5L | 15 | 12.59614 | 5.231288 | 3.343943 | 3.967732 | 10.85565 | 46.09769 | 69.50972 | 140.8862 | -10.5008 | -7.91585 | -9.60928 | -28.6136 | -149.991 | -371.092 | 0.00E+00 | 1.535666 |
| Ip | 16 | -1.55E-08 | 0.419172 | 0.212848 | 0.238377 | 0.551498 | 1.645014 | 1.489633 | 1.53422 | -0.41917 | -0.21285 | -0.23838 | -0.5515 | -1.64501 | -1.48963 | -1.53422 | 0.00E+00 |

| | | OH | PF1AU | PF1bU | PF1cU | PF2U | PF3U | PF4U | PF5U | PF1AL | PF1bL | PF1cL | PF2L | PF3L | PF4L | PF5L | Ip |
|---|---|---|---|---|---|---|---|---|---|---|---|---|---|---|---|---|---|
| MZ | | Influence | Matrix | N-m/rad | | | | | | | | | | | | | |
| OH | 1 | 0.00E+00 | -5784.29 | -2838.07 | -1513.56 | -1616.71 | -1121.45 | -371.817 | -348.327 | 5784.292 | 2838.077 | 1513.561 | 1616.714 | 1121.453 | 371.8189 | 348.3287 | 1.54E-03 |
| PF1AU | 2 | 7.152492 | 0.00E+00 | -73.6636 | -20.0842 | -10.7058 | -1.67E-02 | 1.050949 | 1.221679 | 4.40E-02 | 2.56E-02 | 2.81E-02 | 7.11E-02 | 0.266337 | 0.352855 | 0.613915 | 4.54E-02 |
| PF1bU | 3 | 0.450232 | -6.49832 | 0.00E+00 | -0.48198 | -0.75231 | 0.146579 | 0.101039 | 0.110743 | 3.10E-03 | 1.88E-03 | 2.03E-03 | 5.06E-03 | 1.95E-02 | 2.64E-02 | 4.72E-02 | 2.47E-03 |
| PF1cU | 4 | -4.01E-02 | -1.14453 | -0.29893 | 0.00E+00 | -1.36518 | 0.137595 | 7.59E-02 | 8.12E-02 | 2.03E-03 | 1.17E-03 | 1.35E-03 | 3.36E-03 | 1.35E-02 | 1.80E-02 | 3.27E-02 | 1.64E-03 |
| PF2U | 5 | 3.73E-02 | 3.25E-02 | 8.51E-03 | -3.28E-02 | 0.00E+00 | -2.93E-02 | -9.37E-03 | -9.36E-03 | 1.93E-04 | 4.89E-04 | -2.55E-04 | -2.66E-05 | -5.84E-04 | -1.09E-03 | -2.90E-03 | -5.31E-05 |
| PF3U | 6 | 3.28E-02 | -8.45E-05 | -1.69E-02 | -2.42E-02 | -0.13652 | 0.00E+00 | -0.19286 | -0.17624 | -1.35E-03 | -6.15E-04 | -1.23E-03 | -2.31E-03 | -1.18E-02 | -1.78E-02 | -3.60E-02 | 1.01E-05 |
| PF4U | 7 | 1.81E-03 | 1.45E-02 | 1.02E-02 | 1.26E-02 | 3.48E-02 | 0.208274 | 0.00E+00 | 1.686089 | -8.70E-02 | -8.69E-02 | -8.68E-02 | -8.67E-02 | -8.36E-02 | -7.60E-02 | -5.52E-02 | -8.88E-02 |
| PF5U | 8 | 6.00E-04 | 2.37E-03 | 1.34E-03 | 1.66E-03 | 4.70E-03 | 2.13E-02 | 0.34347 | 0.00E+00 | 3.96E-04 | 9.27E-05 | 2.31E-04 | 5.87E-04 | 4.05E-03 | 4.44E-03 | 1.63E-02 | -6.30E-04 |
| PF1AL | 9 | -7.15235 | -4.34E-02 | -2.57E-02 | -2.80E-02 | -7.17E-02 | -0.2658 | -0.35305 | -0.61401 | 0.00E+00 | 73.66515 | 20.08523 | 10.70527 | 1.58E-02 | -1.05117 | -1.22179 | -4.59E-02 |
| PF1bL | 10 | -0.45037 | -3.05E-03 | -1.71E-03 | -1.99E-03 | -5.31E-03 | -1.96E-02 | -2.65E-02 | -4.71E-02 | 6.498307 | 0.00E+00 | 0.482262 | 0.752478 | -0.14651 | -0.1009 | -0.11069 | -2.63E-03 |
| PF1cL | 11 | 3.99E-02 | -1.98E-03 | -1.10E-03 | -1.35E-03 | -3.52E-03 | -1.34E-02 | -1.81E-02 | -3.26E-02 | 1.14442 | 0.298811 | 0.00E+00 | 1.365146 | -0.13729 | -7.59E-02 | -8.14E-02 | -1.71E-03 |
| PF2L | 12 | -3.69E-02 | -3.48E-04 | -3.97E-04 | 4.51E-05 | -2.21E-04 | 4.78E-04 | 1.18E-03 | 2.56E-03 | -3.21E-02 | -7.84E-03 | 3.30E-02 | 0.00E+00 | 2.88E-02 | 9.07E-03 | 8.70E-03 | -2.28E-04 |
| PF3L | 13 | -3.30E-02 | 1.25E-03 | 9.91E-04 | 1.05E-03 | 2.59E-03 | 1.25E-02 | 1.79E-02 | 3.62E-02 | 3.17E-04 | 1.61E-02 | 2.39E-02 | 0.136112 | 0.00E+00 | 0.193252 | 0.176294 | 5.08E-05 |
| PF4L | 14 | -1.84E-03 | -1.38E-04 | -1.84E-04 | -1.52E-04 | -3.86E-04 | -3.46E-03 | -1.12E-02 | -3.20E-02 | -0.0248 | -1.27E-02 | -3.48E-02 | -0.20831 | 0.00E+00 | -1.68622 | 8.86E-02 | 0.00E+00 |
| PF5L | 15 | -5.71E-04 | -3.25E-04 | -9.78E-05 | -4.88E-04 | -9.94E-04 | -3.86E-03 | -4.33E-03 | -1.58E-02 | -2.34E-03 | -1.28E-03 | -1.46E-03 | -4.74E-03 | -2.13E-02 | -0.34239 | 0.00E+00 | 5.13E-04 |
| Ip | 16 | -4.60E-10 | -1.95E-02 | -1.32E-02 | -1.53E-02 | -4.05E-02 | -0.16181 | -0.22447 | -0.26779 | 1.95E-02 | 1.32E-02 | 1.53E-02 | 4.05E-02 | 0.161809 | 0.224468 | 0.267794 | 0.00E+00 |

## ACKNOWLEDGMENT

The primary author would like to thank the coauthors for their patience in cross checking the influence coefficients reported in this paper. .

## REFERENCES


[1] NSTX Influence Coefficients, calculation # NSTXU 13 03-00, R. Hatcher DATE: July 9 2009

[2] "MHD and Fusion Magnets, Field and Force Design Concepts", R.J.Thome, John Tarrh, Wiley Interscience, 1982.

[3] NSTX-CALC-13-001-00 Rev 1 Global Model – Model Description, Mesh Generation, Results, Peter H. Titus June 2011.

[4] DIGITAL COIL PROTECTION SYSTEM (DCPS) REQUIREMENTS DOCUMENT (DRAFT)**,** NSTX-CSU-RD-DCPS for the National Spherical Torus Experiment Center Stack Upgrade, February 5, 2010 R. Woolley.

[5] OOP PF/TF Torques on TF , R. Woolley, NSTXU CALC 132-03-00

[6] WBS 1.1.3 Structural Analysis of the PF1 Coils Leads and Supports, Rev1 STX-CALC-133-01-01 Prepared By: Leonard Myatt,.

[7] [15]Final Test Report,PPPL Purchase Order PE010637-W Fabrication and Short Beam Shear Testing of Epoxy and Cyanate Ester/Glass Fiber-Copper Laminates April 8, 2011 Prepared for: Princeton Plasma Physics Laboratory Prepared by: Composite Technology Development, Inc.2600 Campus Drive, Suite D Lafayette, CO 80026

The Princeton Plasma Physics Laboratory is operated
by Princeton University under contract
with the U.S. Department of Energy.

Information Services
Princeton Plasma Physics Laboratory
P.O. Box 451
Princeton, NJ 08543

Phone: 609-243-2245
Fax: 609-243-2751
e-mail: pppl_info@pppl.gov
Internet Address: http://www.pppl.gov